Supporting Information

Mimicing Plasmon Nanolaser Emission by Selective Extraction Eletromagnetic Near-Field from Photonic Microcavity

Qian Deng, Meng Kang, Di Zheng, Shunping Zhang, Hongxing, Xu

Sample characterization

Atomic force microscopy (AFM) was used to characterize the heights of the prepared samples after all the optical measurements had been finished. Figure S1 (a) is the AFM image of the hybrid structure. The scanning area is 3.3 μm × 3.3 μm around the silver nanorod. The bright wire-like band on the dark background in the AFM image corresponds to the CdSe nanobelt and its height is 158 nm (Figure S1 (b)). The silver nanorod, shown as a bright rod-like spot on the CdSe nanobelt in the AFM image, shows a small aspect ratio because of the alumina coating with a thickness of 64 nm. Figure S1 (c) is the transmission electron microscope (TEM) image of a typical synthesized silver nanorod. The shadow area in the center of the nanorod corresponds to the gold nanobypyramide.

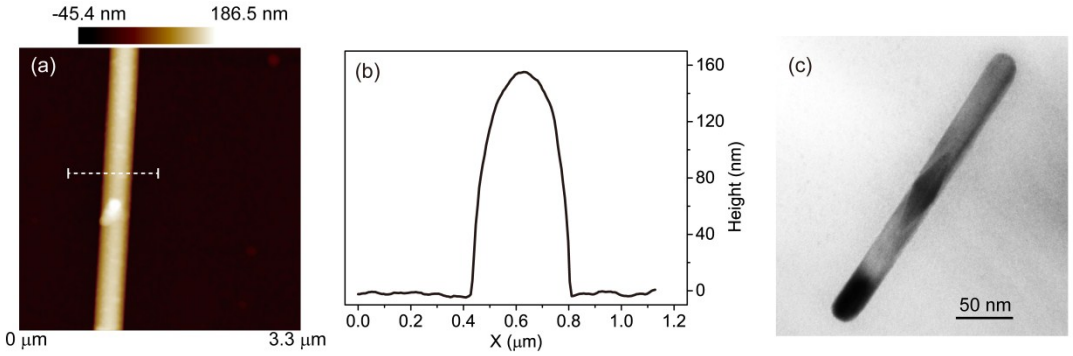

Figure S1. (a) AFM image of the hybrid system. (b) Corresponding height diagram of the section marked as the dotted line in (a). (c) TEM image of the synthesized silver nanorod.

Mode analysis of silver nanorod

A typical dark-field scattering spectra of a silver nanorod with a high aspect ratio on silica substrate is shown in Figure S2 (a). The second (n = 2) and third (n = 3) order mode can be obviously identified, as denoted on top of each peak. The dipole mode (n = 1) locates in the IR range which cannot be detected by our spectrometer. By plotting the resonant wavelength of the silver nanorods as a function of the length of the nanorod in Figure S2 (b), modes of different orders fall into different regions, showing a linear dependent of the resonant wavelength on the length L of the nanorod. In this plot, diameters of the selected silver nanorods are restricted in a tolerable floating range of 25 nm ± 3 nm. Linear fits to the data yield $\lambda_2 = 1.70L + 375.9$ for the second order mode and $\lambda_3 = 1.4L + 269.6$ for the third order mode. This linear dependence of plasmon resonant wavelength on the length of nanorod enables us to identify the mode index n of a silver nanorod with a known size.

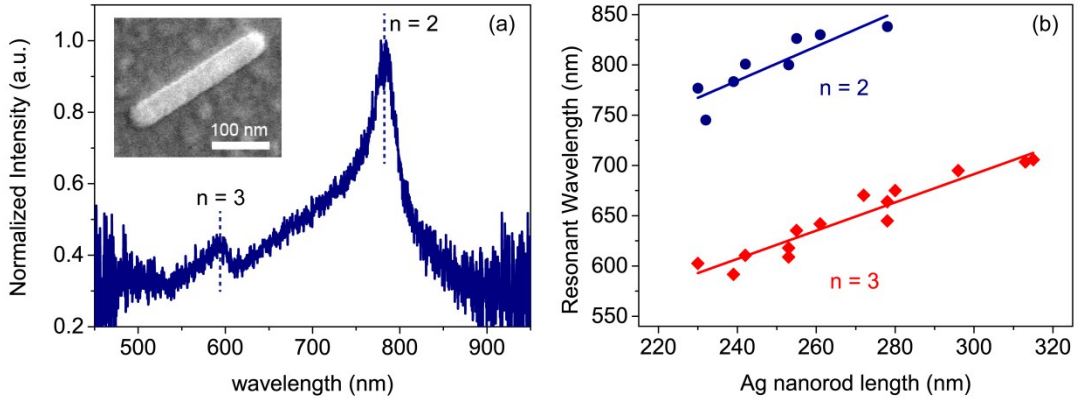

Figure S2. (a) A typical dark-field scattering spectra of a silver nanorod on silica substrate. The inset is a SEM image of the measured silver nanorod with the diameter of 25 nm and the length of 239 nm. A gold film with a thickness of ~ 5 nm have been deposited onto the sample to ensure a proper electrical conductivity required by SEM. (b) Resonant peak positions as a function of the length of silver nanorods.

Dynamical tuning of the plasmon resonant wavelength

After the deposition of silver nanorods onto the CdSe nanobelt, an alumina layer with a thickness of 5 nm was immediately deposited onto the sample to avoid oxidation. The corresponding dark-field spectra of the silver nanorod–insulater–CdSe nanobelt system is shown in yellow line in Figure S3. Two higher order (n = 2, 3) resonant modes can be identified clearly. The broad peak between the two modes can be attributed to the scattering of the intrinsic photonic modes of the CdSe nanobelt. The n = 3 mode of the silver nanorod is far from the fluorescent emission band of the CdSe nanobelt, hence we deposited alumina layers onto the sample by steps to dynamically red shift the third order resonant mode of silver nanorod to approach the energy band of CdSe, as shown in Figure S3(a). This dynamical red-shifting of the plasmon mode is owing to the subsequent tuning of the environmental refractive index by the deposition of dielectric alumina layers. The amount of red-shift gradually decline when the thickness of the dielectric coating increases. Further mode shift is hindered when the dielectric coating exceeds 40 nm, because the thick dielectric shell blocks the further increase in the environmental refractive index when the dielectric coating continues.

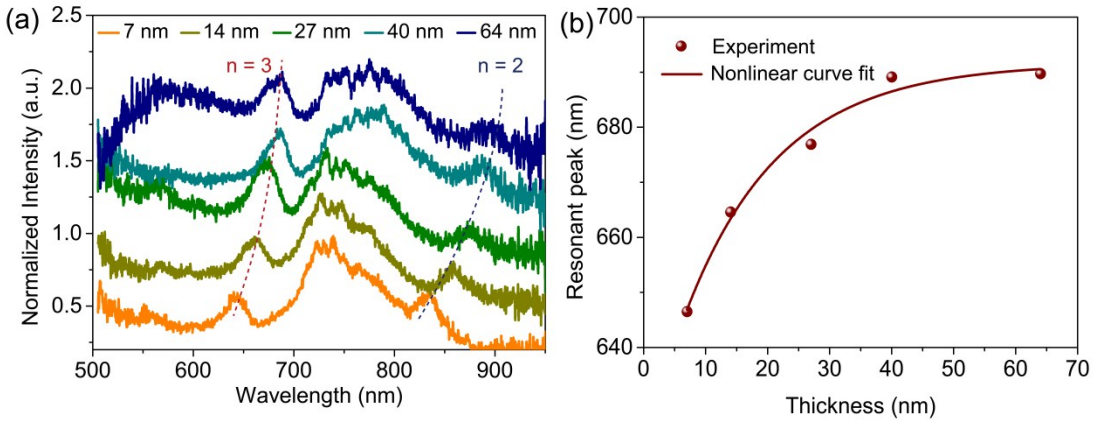

Figure S3. (a) Dark-field scattering spectra of the hybrid system with different thickness of the alumina coating on the silver nanorod. (b) Mode shift as a function of the thickness of the deposited alumina layers.

Dependence of mode spacing on the length of the nanobelt

The optically pumped CdSe nanobelt behaves as a Fabry-Pérot cavity, and the longitudinal mode spacing is consequently governed by the expression: $\Delta\lambda = \lambda^2 / 2Ln_g$, where λ is the wavelength, L is the length of CdSe nanobelt, and n_g is the group index of the system. Thus, the measured photonic laser based on the CdSe nanobelt will follow a linear relationship of $\Delta\lambda$ versus $1/L$. We plotted the FSR of CdSe nanobelts with varying lengths and fit it linearly, demonstrating a group index of ~4.4 for the isolated photonic nanobelt lasing system.

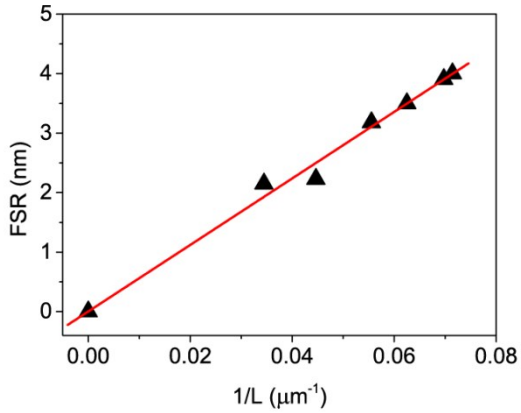

Figure S4. Longitudinal mode spacing versus the inverse of the length of the CdSe nanobelt.

Multimode lasing curves under different pump power densities

A series of photoluminescence spectra under different pump power densities are listed in Figure S4. The red and blue curves correspond to the output emission from CdSe endfacet and silver nanorod, respectively. Under weak pump below threshold (50.3 mW/cm^2), the PL spectrum of the silver nanorod manifest a broadband emission with a peak wavelength of ~ 700 nm, while that of the CdSe endfacet experiences an oscillation, indicating the formation of the Fabry-Pérot cavity mode between the two endfacets of the CdSe nanobelt. When the pump power density is increased to 71.7 mW/cm^2 where the Fabry-Pérot ripples are obviously discernable, amplified spontaneous emission is deemed to start within the photonic cavity of the CdSe nanobelt and the spectrum oscillation emerges on the shoulder of the broad PL background in the emission from the silver nanorod. Further increase in the pump power density results in the accumulation of photons in the cavity mode of CdSe nanobelt, achieving full laser oscillation at both ends. The emission from the silver nanorod is dominated by the narrow lasing peaks consistent with the photonic lasing modes of CdSe nanobelt.

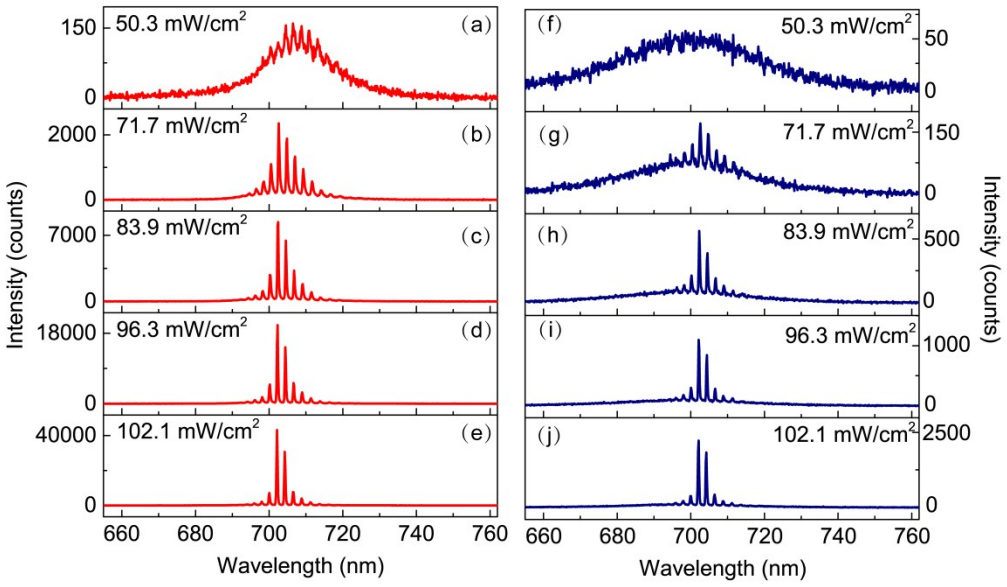

Figure S5. Multimode lasing curves of the same sample depicted in Fig 2. The acquisition areas of the spectra are consistent to that in the maintext. (a) – (e) are the emission spectra of the CdSe endfact under different pump power densities, while (f) – (j) are the corresponding spectra from the silver nanorod.